SAND2020-3321C

Adaptive Protection Scheme for a Real-World Microgrid with 100% Inverter-Based Resources

Trupal Patel
Sukumar Brahma
Holcombe Department of ECE
Clemson University
Clemson, SC, USA
trupalp@clemson.edu
sbrahma@clemson.edu

Javier Hernandez-Alvidrez
Matthew J. Reno
Sandia National Laboratories
Albuquerque, NM, USA
jherna4@sandia.gov
mjreno@sandia.gov

***Abstract*—As more renewable generation connects to distribution systems, it is imminent that existing distribution feeders will be converted to microgrids - systems that offer resilience by providing the flexibility of supporting the grid in normal operation and operating as self-sustained islands when the grid is disconnected. However, inverter control and feeder protection will need to be tuned to the operating modes of the microgrid. This paper offers an insight into the issues involved by taking a case study of a real-world feeder located in the southwestern US that was converted to a microgrid with three solar PV units connecting to the feeder. Different inverter control configurations and adaptive protection using different settings for different operating conditions are proposed for safe operation of this microgrid. The solution also helps to create a framework for protection and coordination of other similar microgrids.**

***Index Terms*—Distribution systems, inverter-based resource (IBR), microgrid, power system protection.**

I. Introduction

There has been a significant push in many parts of the world to start using more renewable energy resources due to rising concerns regarding the environmental effects of fossil-based energy production and the decreasing cost of renewable energy sources. More than half the states in the United States (US) have enacted legislation to increase the share of renewables in their energy mix; for example, Washington DC, California, and Hawaii have increased their Renewable Portfolio Standards (RPS) target to 100% renewable before 2045. Many of the RPS targets also include specific requirements for solar PV based generation to ensure variety in their energy generation [1]. The increase in demand for more sustainable, reliable and resilient power has led to a subset of the power grid known as a microgrid. Microgrids are a combination of generation resources and load, forming an electrically sustainable grid that can function either connected to the larger grid or in an islanded mode. As microgrids gain popularity and distributed generation becomes more commonplace, it is expected that microgrids will be created by adding Distributed Energy Resources (DERs) at the distribution level and converting existing feeders to microgrids. In grid-connected mode, a microgrid shares its load and generation resources, whereas in islanded mode it is disconnected from the utility grid and is self-sufficient. Distribution level microgrids tend to have a significant amount of their energy generation from solar PV and/or storage, which connect through inverters. When multiple inverter-based resources (IBRs) connect to microgrids, their control in grid-connected and islanded modes need to be carefully designed for smooth operation and transition between modes. Due to the distinctly different fault response of IBRs, which includes limiting the positive-sequence current to values comparable to its rated output and blocking of negative-sequence currents, protection of microgrids also needs careful attention.

A wide array of protection schemes have been proposed for microgrids. Each assumes a certain topology, source-type and operating conditions [2]. A summary of such schemes is provided in [3]. The schemes are based on overcurrent, undervoltage, a combination of the two, distance, differential, harmonic-content, and traveling waves, many using various communication infrastructure. Shiles *et al.* [4] provide an overview of the protection methods used in various microgrid projects across North America. Several principles and methods are mentioned based on undervoltage, voltage-restrain, impedance, differential, directional overcurrent and adaptive, some even including fault current limiters. It underscores that the protection methods are highly dependent on the type of sources used in the system, and the system topology. None of the methods discussed has selective protection for an islanded microgrid. Laaksonen *et al.* [5] present an adaptive protection and control scheme using communication, developed for the Hailuoto Island microgrid, where the relay settings are modified depending on the mode of operation. Sources in this case consist of diesel generators and wind turbines. The literature survey reveals that protection schemes suitable for realistic microgrids with 100% IBRs have not been sufficiently explored. Brahma *et al.* [6], [7] provide some insight in to protection of islanded, unbalanced microgrids with 100% IBRs, but do not model a test system with multiple inverters

This work was funded by Sandia National Laboratories, under contract DE-NA0003525, Clemson PO-2004274. Sandia National Laboratories is a multimission laboratory managed and operated by National Technology & Engineering Solutions of Sandia, LLC, a wholly owned subsidiary of Honeywell International Inc., for the U.S. Department of Energy's National Nuclear Security Administration under contract DE-NA0003525.

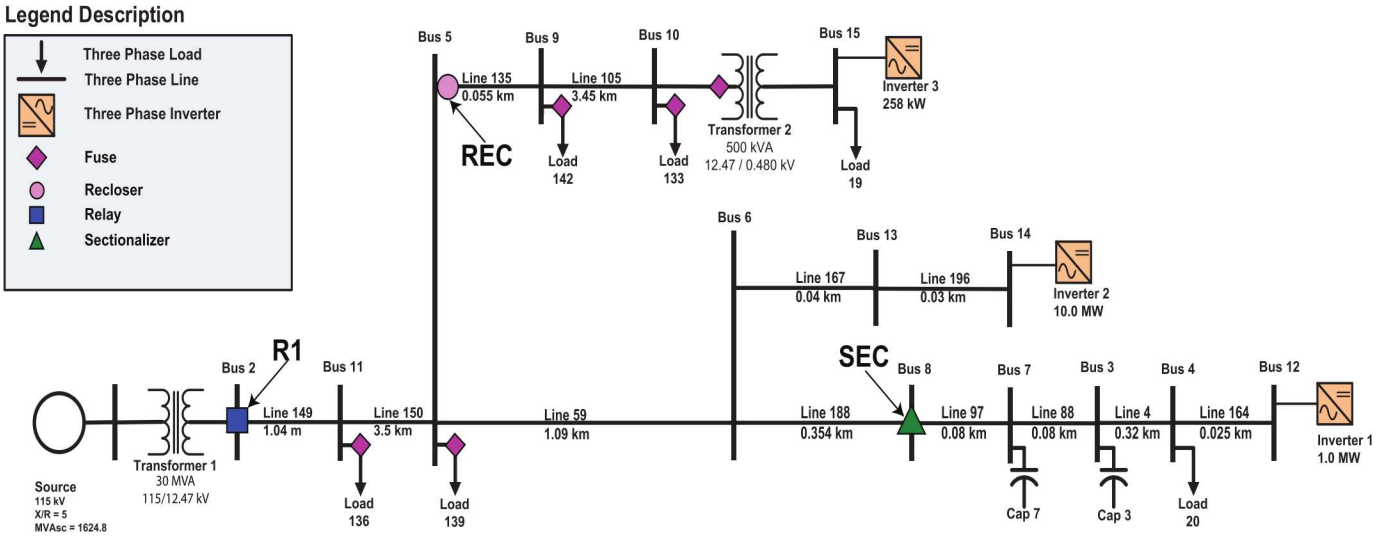

Fig. 1. 12.47kV utility distribution feeder considered for conversion to a microgrid.

to illustrate the control and protection aspects.

This paper models a real-world feeder in the southwestern US with its existing protection. This feeder is being converted to a microgrid by connecting three solar PV units of varying capacity. The paper first proposes inverter controls for operation of microgrids in both operating modes. The controls are designed to mimic the dynamics of commercially available inverters tested at Sandia National Laboratories (SNL). With the controls in place, it then presents protection analysis of the feeder with the existing protection scheme, shows how and why the scheme will not work in the proposed microgrid, and offers an adaptive protection scheme, including selective protection for island, using protective devices available in market today. This exercise, in addition to making the microgrid functional, will create insights and framework that will help design and coordination of protection schemes for other microgrids dominated by IBRs.

II. Test System

The real-world $12.47kV$, 15-bus distribution feeder used for this study is shown in Fig. 1. It is proposed to be converted in to a microgrid by adding PV generation of $258kW, 1MW, 10MW$ at buses $15, 12, 14$ respectively. This feeder has a total load of approximately 3 MVA, so in grid-connected mode the microgrid will feed its load and feed power back to the utility system, all inverters operating at unity power factor. In islanded mode, it will curtail its real power output and supply the required real and reactive power to the microgrid, while maintaining voltage and frequency at acceptable values. Inverters at buses 12 and 14 connect to the system through $480V/12.47kV, YG/YG$ transformers, whereas the inverter at bus 15 connects at 480 V. The system is modeled in Matlab using Simscape power systems library. The grid is molded as a three-phase $115kV$ source connected through a $115kV/12.47kV\Delta/YG$ substation transformer rated at 30MVA. The lines are molded as PI sections. The loads are modeled as Wye-connected constant impedances, which is a valid model for fault-studies.

III. Inverter Control

Two types of control modes are designed for inverter models: grid-following, to be used for grid-connected mode, and grid-forming, to be used in islanded mode.

A. Grid-Following Inverter Model

During the grid-connected mode, the inverters operate in grid-following mode providing the rated or set-point real power to the microgrid, while reactive power is supplied by the utility grid. The grid-following mode inverter-models are based on [8] and [9] as average models using MATLAB's Simscape Electrical Specialized Power Systems library. This mode uses a synchronous reference frame phase locked loop (PLL) to track the voltage and frequency at the inverter's point of common coupling (PCC). The measured voltage is used as the reference by the PLL to synchronize the inverter PI controllers that regulate the injection of real and reactive power at the PCC. The current-limiting feature is implemented with a simple saturation limit on the reference current generated by the current controller, limiting the current to 2 per unit (pu), based on the inverter rating. This limit is consistent with inverters tested at SNL [10]. The reactive support during low voltage ride through (LVRT) is also incorporated as described in [8].

B. Grid-Forming Inverter Model

During islanded conditions, the inverters operate in grid-forming mode, where they provide voltage and frequency regulation for the islanded microgrid to operate properly. In this mode, the real and reactive power injection are based upon the conventional droop characteristics presented in [11]. Also, a virtual impedance current limiting scheme discussed in [12] was used to limit the currents at 2 pu.

IV. Issues With Existing Protection

As per the standard protection methods for distribution feeders. The test feeder is protected using a relay at the substation, a recloser, a sectionalizer, and load fuses, as shown in Fig. 1. Overcurrent (OC) relay $R1$ *with reclosing function* is located at bus 2 and is coordinated with the sectionalizer SEC at bus 8 and the recloser REC at bus 5. The loads are protected using appropriate load fuses. The fuses and relays are set to operate for permanent faults and recloser and sectionalizer are set to save fuses by clearing temporary faults. While these devices adequately protect the feeder while it is only fed by the grid, they cannot protect the proposed microgrid due to reasons summarized in the next sections. For a more detailed discussion, see [13].

A. Bidirectional Current

Multiple sources create bidirectional fault currents, making simple overcurrent based protection difficult to impossible in many situations. For example, the recloser REC is only supposed to operate for faults downstream (buses 9, 10, 15 and load laterals associated with these buses) as per conventional protection. However, when IBR is added at bus 15, that recloser needs to operate also for upstream faults on lines 149 and 150 in order to isolate the IBR from the fault-point. Thus, as the system changes from single-sourced to multi-sourced, the protection also needs to go from simple OC to at least directional OC, often requiring different settings for both directions, because fault current from IBR for upstream faults may be very limited. For example, the recloser REC sees a load current of approximately 30A flowing towards bus 9 from bus 5. However, depending on the fault location and fault resistance the current observed by the recloser can drop to as low as 10 A in the forward direction as the 258kw inverter feeds the fault. Applying the same logic to the rest of the system with three IBRs the existing protection fails to isolate the faults on buses 3,4,5,6,7 and 8. Protection must be enhanced to isolate faults from the IBR-side. Therefore, relays $R2$ and $R4$ shown in Fig. 2 are added to the existing protection scheme. A relay could be added at bus 14 as well but, because the utility had already added an intelligent recloser at bus 13, it was kept there. Bidirectional currents can also make existing devices misoperate. For example, sectionalizer SEC at bus 8 (see Fig. 1), which previously operated in conjugation with the relay $R1$, cannot be coordinated with two more reclosers REC and IR for faults downstream of SEC. Therefore, it is removed and replaced with a directional overcurrent relay $R3$ to provide better selectivity to the proposed protection.

B. Low Fault current

Since IBRs limit their current output to low values (2 pu in this study), they pose challenges for device coordination in both grid-connected and islanded modes, especially in islanded mode, due to lack of adequate fault currents. For example, the maximum fault current in grid-connected mode for the feeder is around 8000 A. However, the majority of the fault current in grid-connected mode is from the grid. The fault current contribution from the inverters is limited to a maximum of 93 A, 925 A and 24 A for the 1MW, 10 MW and 258kW inverters, respectively. Low fault current from the inverters creates challenges in fault detection from the inverter side as the fault current from the inverters can be similar to load current. The maximum fault current in the islanded mode is reduced by roughly 880 A. The low fault current during islanded mode can lead to difficulties in fault detection or long tripping times for OC elements if set for grid-connected mode. On the other hand, if set for the low fault currents in islanded mode, the OC element could misoperate and fail to coordinate properly in the grid-connected mode.

C. Large coordination ranges

Due to the limited fault currents from IBRs, coordination ranges can become large and lead to difficulties in coordination, often resulting in excessive operating time, as illustrated in [13]. In the test case under discussion, the coordination range for REC can span from 3500 A to 120 A due to large differences in fault current profiles in grid-connected and islanded modes.

V. Proposed Protection Method

It is clear from the discussion in Section IV that bidirectional protective devices are needed to protect the microgrid. It is also clear that settings will need to be different for different operating modes due to a large difference in fault currents, thus requiring an adaptive design. Based on the available protective devices the microgrid is proposed to be divided into 5 protection zones as shown in Fig. 2. Relays $R1$, $R2$, and reclosers REC and IR will have different settings for different fault-current directions. Also, all devices will have different settings for grid-connected mode and islanded mode. For the purpose of this discussion the direction downstream of the feeder will be called ”forward” and the direction upstream ”reverse”. Numerical relay manufactures have relays and other protective devices that can store multiple settings which can be activated and deactivated using communication. These relays also allow the user to create the logic which is used to generate a trip signal based on the output of different relaying elements such as inverse-time overcurrent, under-voltage and directional. Therefore, a relay can be set to operate, for example, if the directional element indicates a forward current *and* the OC criteria are met, *and* the voltage has dropped below the set threshold. Using these programmable trip conditions and multiple group settings the same relay could be adaptively programmed to operate differently for different modes of operation.

A minimum of 2 setting groups should be stored in a relay, 1 for grid-connected mode and 1 for islanded mode. Each setting group is further broken down in to settings for forward (F) and reverse (R) direction. This results in 4 sets of Minimum Operating Current (MOC) settings and Time Dial (TDs) settings for each device that needs to operate for fault current in both directions as shown in figure 3.

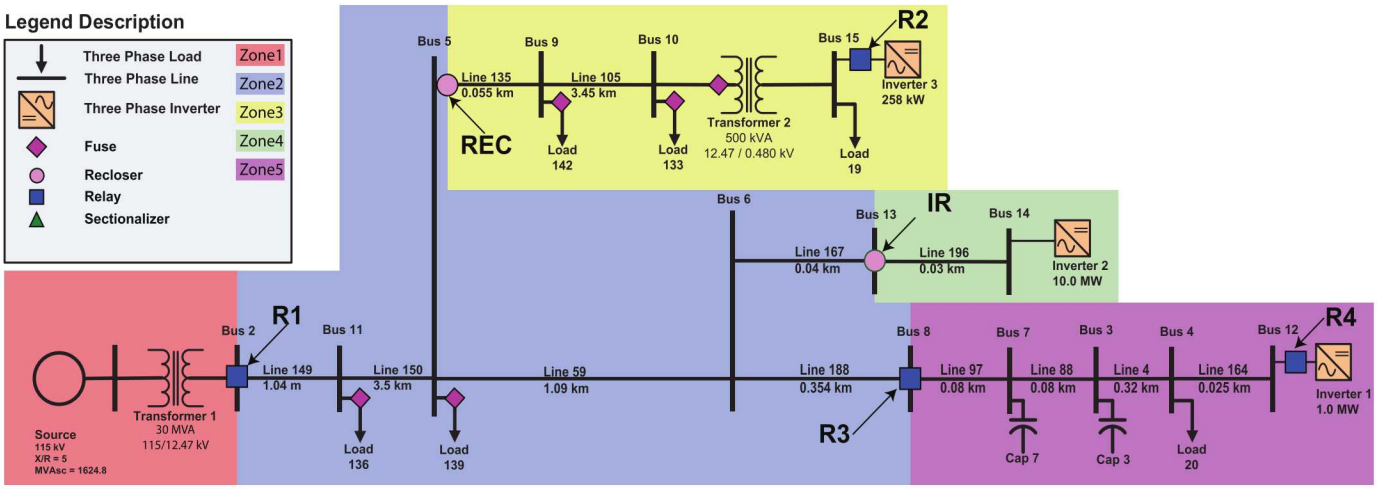

Fig. 2. Utility feeder converted to microgrid with updated protection devices and highlighted zones of protection.

Depending on the microgrid operating mode, either the grid-connected or islanded mode settings will be active. The signal used to switch the inverter operating mode can be used to activate/deactivate the appropriate mode-setting. Example settings for recloser REC are shown in Table I. A recloser has both fast and slow action and their corresponding setting group. For a fault on bus 10 in grid-connected mode, the fault current seen by the recloser is in the forward direction and has a magnitude of roughly 1450 A. In this situation, settings corresponding to mode *GC* and direction *F* in the table will be activated, which translates to MOC of 80 A, and TDS of 10 and 0.5 for the fast and slow curves, respectively. The inverse time OC element will activate when the current exceeds the MOC and will trip after a time delay dictated by the TDS setting.

TABLE I
EXAMPLE SETTINGS FOR RECLOSER REC AT BUS 5

Group #	Mode	Direction	MOC (A)	TDS	Curve
Slow Settings					
1	GC	F	80	10.0	EI
1	GC	R	5	10.0	STI
2	IS	F	53	5.50	IE
2	IS	R	5	7.25	STI
Fast Settings					
1	GC	F	80	0.5	EI
1	GC	R	5	1.57	STI
2	IS	F	53	0.5	IE
2	IS	R	5	1.02	STI

The process of coordination was largely automated using GNU parallel on Clemson University's palmetto cluster computing system. Automation included paralleling of fault analysis for different types of faults in all operating modes, using the minimum and maximum fault current values from the fault analysis to determine pickup current for each device (higher than maximum load current and lower than minimum fault current) and time dial settings for main and backup devices for faults in each zone.

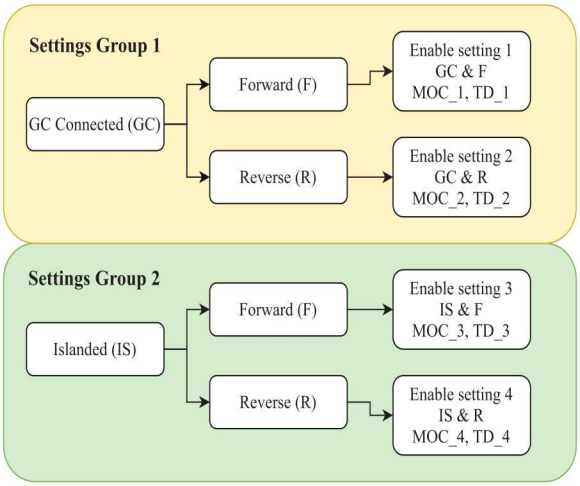

Fig. 3. Settings groups for bidirectional protective devices.

In grid-connected mode, there are two options for isolating faults inside the microgrid. Relay $R1$ can be set to operate instantaneously to disconnect the grid, transitioning the microgrid into islanded mode, and isolating the faulted zone based on settings for the islanded mode. Alternatively, $R1$ can coordinate with the devices inside the microgrid to isolate the faulted zone. The first option is more likely, as utilities do not coordinate with protection of customer-owned systems. However, as microgrids proliferate, it is likely that microgrids may be owned by utilities, in which case, the second option may become feasible. Both options will be discussed here. For the second option, for the microgrid under study, $R1$ will backup $R3$, IR and REC for faults in zones 5, 4, and 3, respectively.

A. Grid-Connected Mode

In the grid-connected mode, zone 1 represents the grid and thus any fault in zone 1 is detected by the PCC controller (using reverse setting of $R1$) and the microgrid is instanta-

neously disconnected from the grid and switched to islanded mode with appropriate protection settings. For any faults in zone 2 the fault is isolated by the combined operation of REC, IR, $R3$ on their respective reverse settings. REC is backed up by $R2$, and $R3$ is backed up by $R4$. The microgrid is isolated by the forward operation of $R1$. For a Fault in zone 3, the fault is isolated by the forward operation of REC followed by operation of $R2$. REC is backed up by the reverse operation of IR and $R3$, and forward operation of $R1$. The coordination plot for zone 3 can be seen in Fig. 4. The dashed line represents the fast-acting curve for the reclosers and vertical lines represent the coordination ranges for the devices. For example, the black vertical lines show that $R1$ backs up the slow curve of REC across the coordination range of 474 A and 1500 A. For the unusual case of coordinating two reclosers REC and IR, the fast curve of IR backs up the fast curve of REC and the slow curve of IR backs the slow curve of REC. If the fast curve of IR is used to back the slow curve of REC, the fault clearing times increase significantly. The device-curves and the coordination ranges are shifted in order to compensate for the fact that different devices see different fractional amounts of the total fault current. A Fault in zone 4 is isolated by the forward operation of IR, backed up by the reverse operation of REC, $R3$ and the forward operation of $R1$. A Fault in zone 5 is isolated by the forward operation of $R3$ and operation of $R4$. $R3$ is backed up by the reverse operation of REC and IR and forward direction of $R1$. Table II shows the operating times (OT) for primary and backup devices for faults at all buses in grid-connected mode.

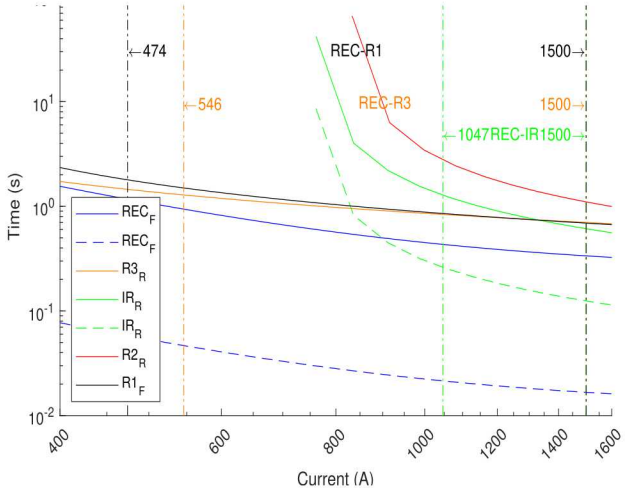

Fig. 4. Zone 3 coordination plot for grid-connected mode.

B. Islanded mode

In islanded mode, all fault contributions are from IBRs operating in grid-forming mode, each providing at the most 2 pu fault current, drastically reducing the fault currents and thus requiring reductions in minimum operating currents (MOC) used by devices to detect faults in the microgrid. For example, the pickup current for REC for faults in zone 3 is 80 A in grid-connected mode but reduces to 53 A in islanded mode. Main and backup devices will remain the same as proposed for grid-connected mode, but with different settings as well as the exclusion of $R1$. The coordination plot for zone 2 can be seen in Fig. 5, with the device curves adjusted. For a fault in zone 2 REC sees a fault current between 15A-20 A, whereas IR sees a fault current between 550A-825 A, so all the curves are shifted to align with the REC curve. Table III shows the operating times for primary and backup devices for all fault locations in islanded mode. All faults are isolated in less than 2.5 s by primary protection, higher clearing times were due to coordination at very low fault currents being required. All fault locations are covered by protective devices. Fuse saving was also achieved when possible for faults on the load laterals. It is clear that the fault clearing times are unconventionally large in many cases, especially for backup protection, but the fault currents in feeders in those cases were also unconventionally

TABLE II
OPERATING TIMES FOR A 3PH FAULT AT ALL BUSES DURING GRID-CONNECTED OPERATION [a,b]

Bus Zone	*Main Device*	*OT (s)*	*Backup Device*	*OT (s)*	*Backup Device*	*OT (s)*
2	REC_R	0.16, 1.11	$R2_R$	6.22		
Z2	IR_R	0.25, 1.22				
	$R3_R$	1.26	$R4_R$	2.24		
	$R1_F$	0.03				
11	REC_R	0.16, 1.11	$R2_R$	6.22		
Z2	IR_R	0.25, 1.22				
	$R3_R$	1.26	$R4_R$	2.23		
	$R1_F$	0.03				
5	REC_R	0.16, 1.11	$R2_R$	1.12		
Z2	IR_R	0.07, 1.19				
	$R3_R$	1.30	$R4_R$	2.04		
	$R1_F$	0.03				
6	REC_R	0.15, 1.02	$R2_R$	1.23		
Z2	IR_R	0.18, 0.88				
	$R3_R$	0.73	$R4_R$	2.24		
	$R1_F$	0.03				
13	REC_R	0.15, 1.04	$R2_R$	1.3		
Z2	IR_R	0.18, 0.88				
	$R3_R$	0.73	$R4_R$	2.24		
	$R1_F$	0.03				
8	REC_R	0.16, 1.09	$R2_R$	1.3		
Z2	IR_R	0.18, 0.88				
	$R3_R$	0.73	$R4_R$	2.25		
	$R1_F$	0.03				
5	REC_F	0.03	IR_R	0.21, 1.02	$R3_R$	0.77
Z3	$R2_R$	1.23				
9	REC_F	0.03	IR_R	0.21, 1.02	$R3_R$	0.77
Z3	$R2_R$	1.23				
10	REC_F	0.03, 0.35	IR_R	0.25, 1.22	$R3_R$	1.29
Z3	$R2_R$	0.69				
15	$FT2$	0.9	REC_F	0.15, 2.93		
Z3	$R2_R$	0.62				
13	IR_F	0.03	REC_R	0.15, 1.04	$R3_R$	0.73
Z4						
14	IR_F	0.03	REC_R	0.15, 1.04	$R3_R$	0.73
Z4						
8	$R3_F$	0.31	IR_R	0.18, 0.88	REC_R	0.16, 1.08
Z5	$R4_R$	2.24				
7	$R3_F$	0.31	IR_R	0.18, 0.88	REC_R	0.16.1.08
Z5	$R4_R$	2.24				
3	$R3_F$	0.31	IR_R	0.18, 0.88	REC_R	0.16, 1.08
Z5	$R4_R$	2.24				
4	$R3_F$	0.31	IR_R	0.18, 0.88	REC_R	0.17, 1.17
Z5	$R4_R$	2.24				
12	$R3_F$	0.31	IR_R	0.18, 0.88	REC_R	0.18, 1.25
Z5	$R4_R$	2.24				

[a] F - Forward Direction, R - Reverse direction.
[b] #,# - Represents recloser operating times for fast,slow actions.

small. The fault current values in lines for such cases did not exceed 1.8 times the maximum load current values observed in the lines. This obviates the possibility of equipment-damage.

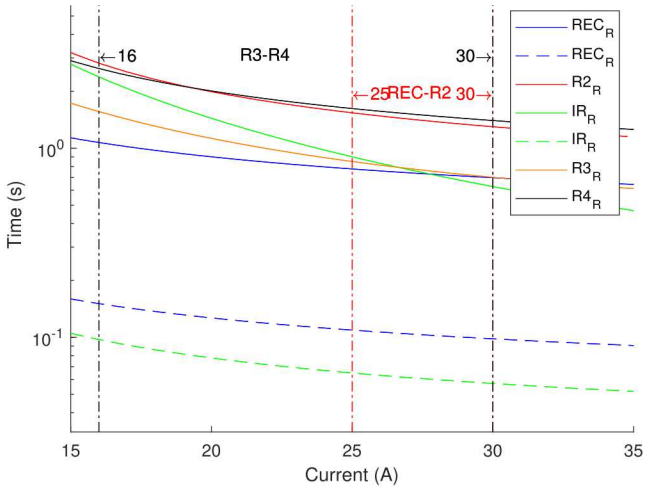

Fig. 5. Zone 2 coordination plot for islanded mode.

VI. Conclusion

The paper explores the challenges faced when converting an existing real-world feeder to an IBR-fed microgrid from a control and protection perspective. An adaptive protection solution is proposed with the constraint of using off-the-shelf equipment and no communication. Results show that the solution works well under the unusual fault profile. This study may be used as a guideline for other similar cases. The number of protective devices to be used and number of zones to be created have an obvious cost-benefit trade-off. The success of the scheme also heavily depends on the fault current limits imposed by inverters. Considering the extensive exercise that was needed for a relatively small system, more complex systems are most likely to require more sophisticated solutions involving communications.

TABLE III
Operating times for a 3ph fault at all Buses During Islanded Operation[a,b]

Bus Zone	*Main Device*	*OT(s)*	*Backup Device*	*OT (s)*	*Backup Device*	*OT (s)*
2	REC_R	0.18, 1.33	$R2_R$	1.5		
Z2	IR_R	0.07, 1.26				
	$R3_R$	1.81	$R4_R$	2.13		
11	REC_R	0.17, 1.24	$R2_R$	1.47		
Z2	IR_R	0.07, 1.26				
	$R3_R$	1.81	$R4_R$	2.23		
5	REC_R	0.17, 1.17	$R2_R$	1.53		
Z2	IR_R	0.07, 1.19				
	$R3_R$	1.30	$R4_R$	2.04		
6	REC_R	0.17, 1.17	$R2_R$	1.53		
Z2	IR_R	0.07, 1.12				
	$R3_R$	1.12	$R4_R$	1.95		
13	REC_R	0.17, 1.17	$R2_R$	1.53		
Z2	IR_R	0.07, 1.12				
	$R3_R$	1.12	$R4_R$	1.95		
8	REC_R	0.17, 1.17	$R2_R$	1.53		
Z2	IR_R	0.07, 1.12				
	$R3_R$	1.23	$R4_R$	1.95		
5	REC_F	0.03, 0.35	IR_R	0.07, 1.17	$R3_R$	1.30
Z3	$R2_R$	1.53				
9	REC_F	0.03, 0.35	IR_R	0.07, 1.19	$R3_R$	1.29
Z3	$R2_R$	1.53				
10	REC_F	0.04, 0.38	IR_R	0.07, 1.27	$R3_R$	1.30
Z3	$R2_R$	1.53				
15	$FT2$	2.55	REC_F	0.10, 6.72		
Z3	$R2_R$	1.73				
13	IR_F	0.09, 0.57	REC_R	0.17, 1.17	$R3_R$	1.1225
Z4						
14	IR_F	0.09, 0.57	REC_R	0.17, 1.17	$R3_R$	1.1225
Z4						
8	$R3_F$	0.38	IR_R	0.07, 1.27	REC_R	0.17, 1.17
Z5	$R4_R$	1.95				
7	$R3_F$	0.38	IR_R	0.07, 1.12	REC_R	0.17, 1.17
Z5	$R4_R$	1.95				
3	$R3_F$	0.38	IR_R	0.07, 1.12	REC_R	0.17, 1.17
Z5	$R4_R$	1.95				
4	$R3_F$	0.38	IR_R	0.07, 1.19	REC_R	0.17, 1.17
Z5	$R4_R$	1.95				
12	$R3_F$	0.38	IR_R	0.07, 1.19	REC_R	0.17, 1.17
Z5	$R4_R$	1.95				

[a] F - Forward Direction, R - Reverse direction.
[b] #,# - Represent recloser operating times for fast,slow actions.

References

[1] G. L. Barbose, "U.S. Renewables Portfolio Standards: 2019 Annual Status Update," Lawrence Berkeley National Laboratory, Tech. Rep., Jul. 2019. [Online]. Available: https://emp.lbl.gov/projects/renewables-portfolio

[2] S. S. Venkata, M. Reno, W. Bower, S. Manson, J. Reilly, and G. W. Sey Jr, "Microgrid protection: Advancing the state of the art," Sandia National Laboratorie, Tech. Rep., 03 2019.

[3] A. R. Haron, A. Mohamed, and H. Shareef, "A review on protection schemes and coordination techniques in microgrid system," *Journal of Applied Sciences*, vol. 12, pp. 101–112, 02 2012.

[4] J. Shiles, E. Wong, S. Rao, C. Sanden, M. A. Zamani, M. Davari, and F. Katiraei, "Microgrid protection: An overview of protection strategies in north american microgrid projects," in *2017 IEEE Power Energy Society General Meeting*, July 2017, pp. 1–5.

[5] H. Laaksonen, D. Ishchenko, and A. Oudalov, "Adaptive protection and microgrid control design for hailuoto island," *IEEE Transactions on Smart Grid*, vol. 5, no. 3, pp. 1486–1493, May 2014.

[6] S. Brahma, N. Pragallapati, and M. Nagpal, "Protection of islanded microgrid fed by inverters," in *2018 IEEE Power Energy Society General Meeting (PESGM)*, Aug 2018, pp. 1–5.

[7] S. Brahma, "Protection of distribution system islands fed by inverter-interfaced sources," in *2019 IEEE Milan PowerTech*, June 2019, pp. 1–6.

[8] R. Teodorescu, M. Liserre, and P. Rodriguez, *Grid converters for photovoltaic and wind power systems*. Wiley, 2011.

[9] J. Hernandez-Alvidrez, A. Summers, N. Pragallapati, M. J. Reno, S. Ranade, J. Johnson, S. Brahma, and J. Quiroz, "PV-inverter dynamic model validation and comparison under fault scenarios using a power hardware-in-the-loop testbed," in *2018 IEEE 7th World Conference on Photovoltaic Energy Conversion (WCPEC)*, June 2018, pp. 1412–1417.

[10] N. Gurule, J. Hernandez-Alvidrez, M. Reno, A. Summers, S. Gonzalez, and J. Flicker, "Grid-forming inverter experimental testing of fault current contributions," in *IEEE Photovoltaic Specialists Conference (PVSC)*, 06 2019.

[11] J. Hernandez-Alvidrez, A. Summers, M. Reno, J. Flicker, and N. Pragallapati, "Simulation of grid-forming inverters dynamic models using a power hardware-in-the-loop testbed," in *2019 IEEE Photovoltaic Specialists Conference (PVSC)*, 06 2019.

[12] A. Gkountaras, S. Dieckerhoff, and T. Sezi, "Evaluation of current limiting methods for grid forming inverters in medium voltage microgrids," in *2015 IEEE Energy Conversion Congress and Exposition (ECCE)*, Sep. 2015, pp. 1223–1230.

[13] S. M. Brahma, J. Trejo, and J. Stamp, "Insight into microgrid protection," in *IEEE PES Innovative Smart Grid Technologies, Europe*, Oct 2014, pp. 1–6.